nature neuroscience

SUPPLEMENTARY INFORMATION

https://doi.org/10.1038/s41593-019-0419-y

In the format provided by the authors and unedited.

Sensory lesioning induces microglial synapse elimination via ADAM10 and fractalkine signaling

Georgia Gunner[1], Lucas Cheadle[2,9], Kasey M. Johnson[1,9], Pinar Ayata[3,4], Ana Badimon[3], Erica Mondo[1], M. Aurel Nagy[2], Liwang Liu[1], Shane M. Bemiller[5], Ki-Wook Kim[6], Sergio A. Lira[7], Bruce T. Lamb[5], Andrew R. Tapper[1], Richard M. Ransohoff[8], Michael E. Greenberg[2], Anne Schaefer[3,4] and Dorothy P. Schafer[1]*

[1]Department of Neurobiology, Brudnick Neuropsychiatric Research Institute, University of Massachusetts Medical School, Worcester, MA, USA. [2]Department of Neurobiology, Harvard Medical School, Boston, MA, USA. [3]Fishberg Department of Neuroscience, Department of Psychiatry, Friedman Brain Institute, Icahn School of Medicine at Mount Sinai, New York, NY, USA. [4]Ronald M. Loeb Center for Alzheimer's Disease, Icahn School of Medicine at Mount Sinai, New York, NY, USA. [5]Stark Neurosciences Research Institute, Indiana University, Indianapolis, IN, USA. [6]Department of Pharmacology and Center for Stem Cell and Regenerative Medicine, University of Illinois College of Medicine, Chicago, IL, USA. [7]Precision Immunology Institute, Icahn School of Medicine at Mount Sinai, New York, NY, USA. [8]Third Rock Ventures, Boston, MA, USA. [9]These authors contributed equally: Lucas Cheadle, Kasey M. Johnson. *e-mail: Dorothy.schafer@umassmed.edu

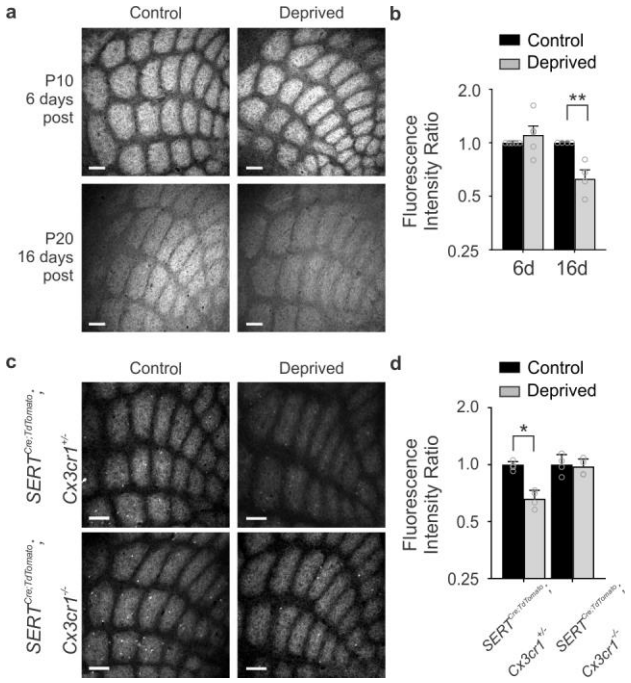

Supplementary Figure 1

TC input elimination is observed following whisker trimming and with genetic labeling of TC inputs.

a, Daily whisker trimming from P4 results in decreased barrel fluorescence intensity by day 16 (bottom panels), but no by day 6 (top panels). Scale bar, 150 µm. **b,** Quantification for barrel fluorescence intensity in a (Two-way ANOVA with Sidak's post hoc, 6-day control vs trimmed, n = 5 animals, $P = 0.5093$, $t = 1.078$, $df = 14$; 16-day control vs trimmed, n = 4 animals, $P = 0.0071$, $t = 3.496$, $df = 14$). Data are normalized to the control barrel cortex within the same animal for each timepoint. **c,** TC inputs labeled by transgenic expression of tdTomato are eliminated in the deprived barrel cortex in a CX3CR1-dependent manner following whisker lesioning by cauterization. Representative tangential sections of *Sert*-Cre tdTomato labeled TC inputs within layer IV of the control and deprived barrel cortices of *Cx3cr1*$^{+/-}$ (top row) and *Cx3cr1*$^{-/-}$ (bottom row) mice 7 d post-sensory deprivation. Scale bar, 150 µm. **d**, There is a significant decrease in TC inputs as measured by fluorescence intensity of tdTomato signal in the deprived (gray bars) vs. the contralateral control (black bars) barrel cortex in *Cx3cr1*$^{+/-}$ mice 7 d-post deprivation. No significant decrease in fluorescence was observed in *Cx3cr1*$^{-/-}$ mice. Data are normalized to the control barrel cortex for each genotype. (Two-Way ANOVA with Sidak's post hoc, n=4 animals per genotype, *Cx3cr1*$^{+/-}$ control vs deprived, $P = 0.0405$, $t = 2.668$, $df = 12$; *Cx3cr1*$^{-/-}$ control vs deprived, $P = 0.9808$, $t = 0.1782$, $df = 12$.) All data presented as mean ± SEM.

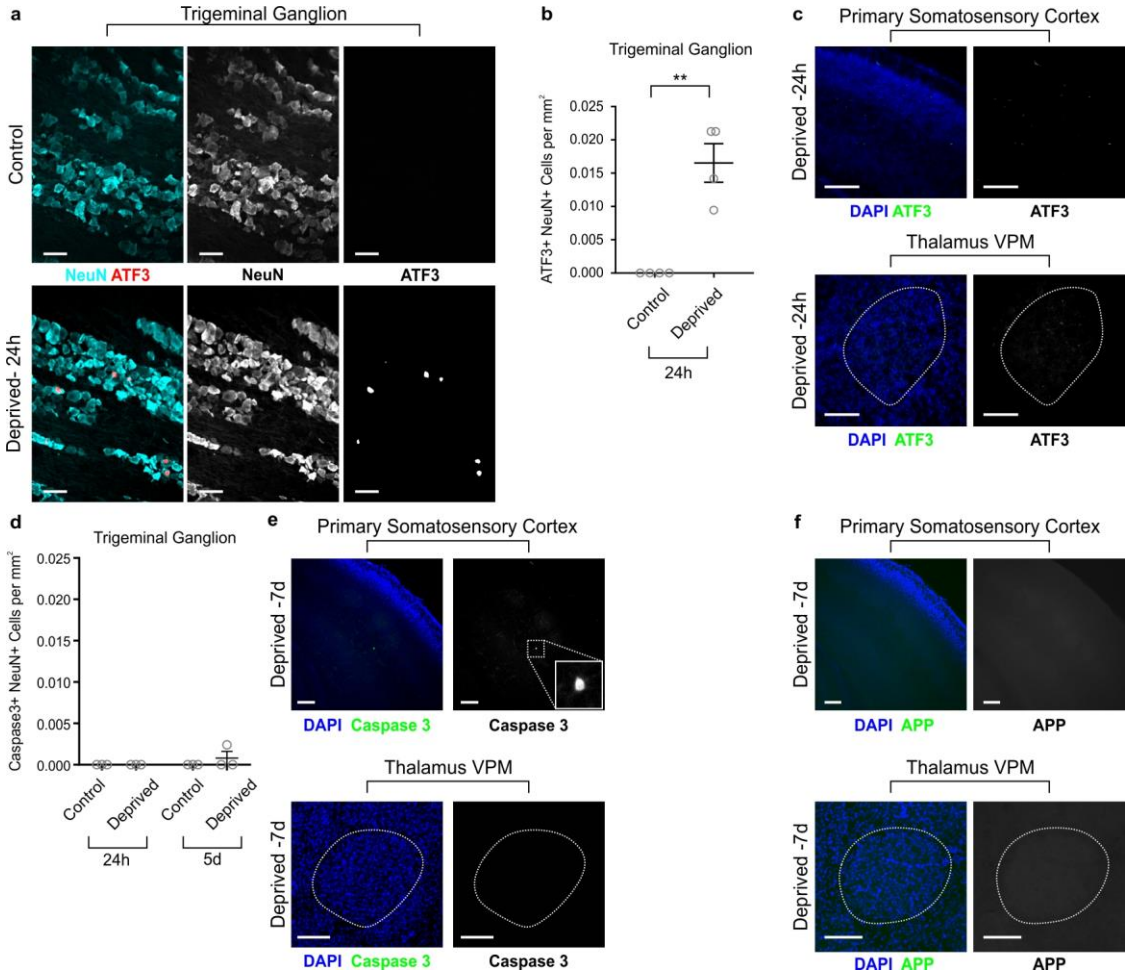

Supplementary Figure 2

Effects of whisker lesioning at P4 on cell death, axon degeneration, and cell stress in the barrel cortex circuit.

a, Immunostaining of trigeminal ganglia, which contain the neurons that innervate the whisker follicles. There is a significant increase in ATF3 (red, marker of cell stress) in NeuN-positive neurons (cyan) at 24h post whisker lesioning (deprived, bottom row). Scale bar, 50 µm. **b**, Quantification for ATF3 signal co-localized to NeuN in the control and deprived trigeminal ganglia. (Two-tailed Student's t-Test, n = 4 animals; $P = 0.0012$, $t = 5.715$, $df = 6$). **c**, Representative images from 3 animals show ATF3 signal (green) is not detected in the ventral posterior medial nucleus (VPM) of the thalamus (bottom panels; dotted line borders the VPM) nor the primary somatosensory cortex (top panels) 24 hours after whisker lesioning. Scale bars, 150 µm. **d**, Quantification for cell death marker cleaved caspase 3 shows cell death does not occur 24h nor 5d after whisker lesioning in the trigeminal ganglia. (Two-way ANOVA with Sidak's post hoc, 24h control vs deprived, n = 3 animals, $P > 0.9999$, $t = 0$, $df = 8$; 6d control vs deprived, n = 3 animals, $P = 0.3520$, $t = 1.414$, $df = 8$). Data presented as mean ± SEM. **e-f**, Representative images from 3 animals for the deprived somatosensory cortex and VPM 7 days after whisker lesioning in control mice shows no increased cell death (e; caspase 3, green) nor axon degeneration (f; APP, green) in either brain region. Scale bars, 150 µm.

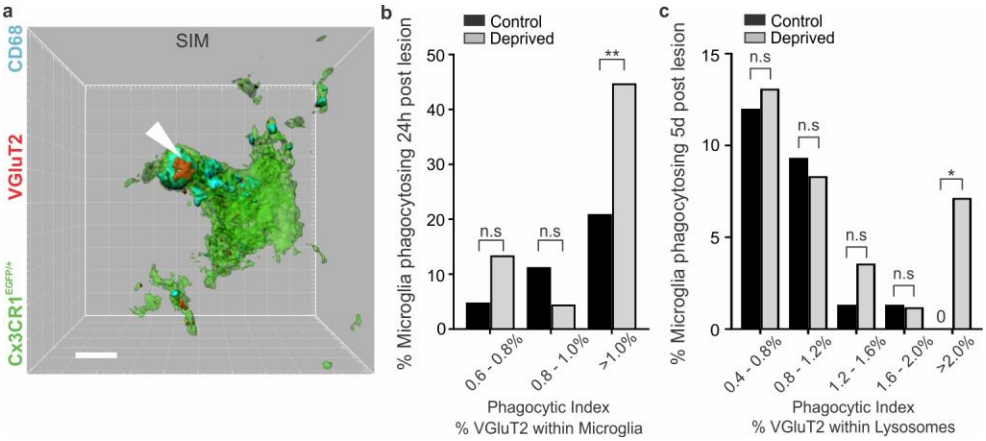

Supplementary Figure 3

Super resolution imaging reveals TC inputs are internalized within microglia following sensory deprivation.

a, Structured illumination microscopy (SIM) of a microglia (CX3CR1$^{EGFP/+}$, green) which has engulfed VGluT2-positive TC presynaptic inputs (red) within its lysosomes (anti-CD68, cyan) in the deprived barrel cortex 24 h after whisker removal. Scale bar, 5 µm. **b-c**, Quantification of the % of microglia out of the total microglial population phagocytosing VGluT2-positive inputs 24h (b) and 5d (c) after whisker lesioning in the control (black bars) and deprived (grey bars) cortices. Microglia in the deprived cortex both 24h and 5d after lesioning have a higher proportion of cells with a high phagocytic index (b, >1.0%; c, >2.0%) compared to the control cortex (24h: n = 129 cells; Two-Sided Fisher's Exact Test; for 0.6-0.8%; *P* = 0.1306; for 0.8-1.0%; *P* = 0.1941; for >0.1%, *P* = 0.0051; 5d: n = 159 cells; Two-Sided Fisher's Exact Test; for 0.4-0.8%; *P* >0.9999; for 0.8-1.2%; *P* >0.9999; for 1.2-1.6%; *P* = 0.6227; for 1.6-2.0%; *P* >0.9999; for >2.0% *P* = 0.0298). Data represented as whole number percentage of the total cell population.

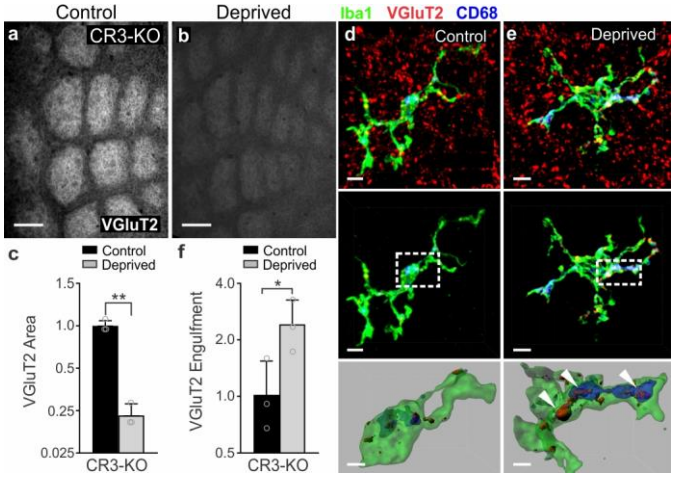

Supplementary Figure 4

CR3 is not required for whisker lesion-induced TC input engulfment and elimination.

a,b, Representative images of VGluT2 immunoreactivity in the non-deprived (a) and deprived (b) barrel cortices of CR3-KO mice show TC inputs are properly eliminated 6 d after whisker lesioning. Scale bar, 150 µm. **c**, Quantification of VGluT2 area within barrel centers 7 d after whisker removal reveals that TC inputs are still eliminated in CR3-KO mice. (Data normalized to the control, non-deprived VGluT2 area within each animal; Two-tailed Student's t-test, n = 3 animals, P = 0.0015, t =7.765 df =4). **d,e**, Top Panels, Fluorescent images of microglia within the control (d) and deprived (e) barrels of CR3-KO mice. Scale bar, 5 µm. Middle panels depict VGluT2 signal (red) within microglia (green) and within lysosomes (blue). Bottom panels are 3D surface-rendered insets (dotted boxes in middle panels) of control (d) and deprived (e) CR3-KO microglia. Arrows depict increased VGluT2 internalization within microglia in the deprived hemisphere. Scale bar, 2 µm. **f**, Quantification of VGluT2 engulfment within CR3-KO microglia 24 h after whisker removal reveals that CR3 deficiency fails to block microglial engulfment of TC inputs. (Data normalized to engulfment in microglia in the control hemisphere within each animal; Two-tailed Student's t-test, n = 3 animals, P = 0.260, t =4.215 df =2). All data presented as mean ± SEM.

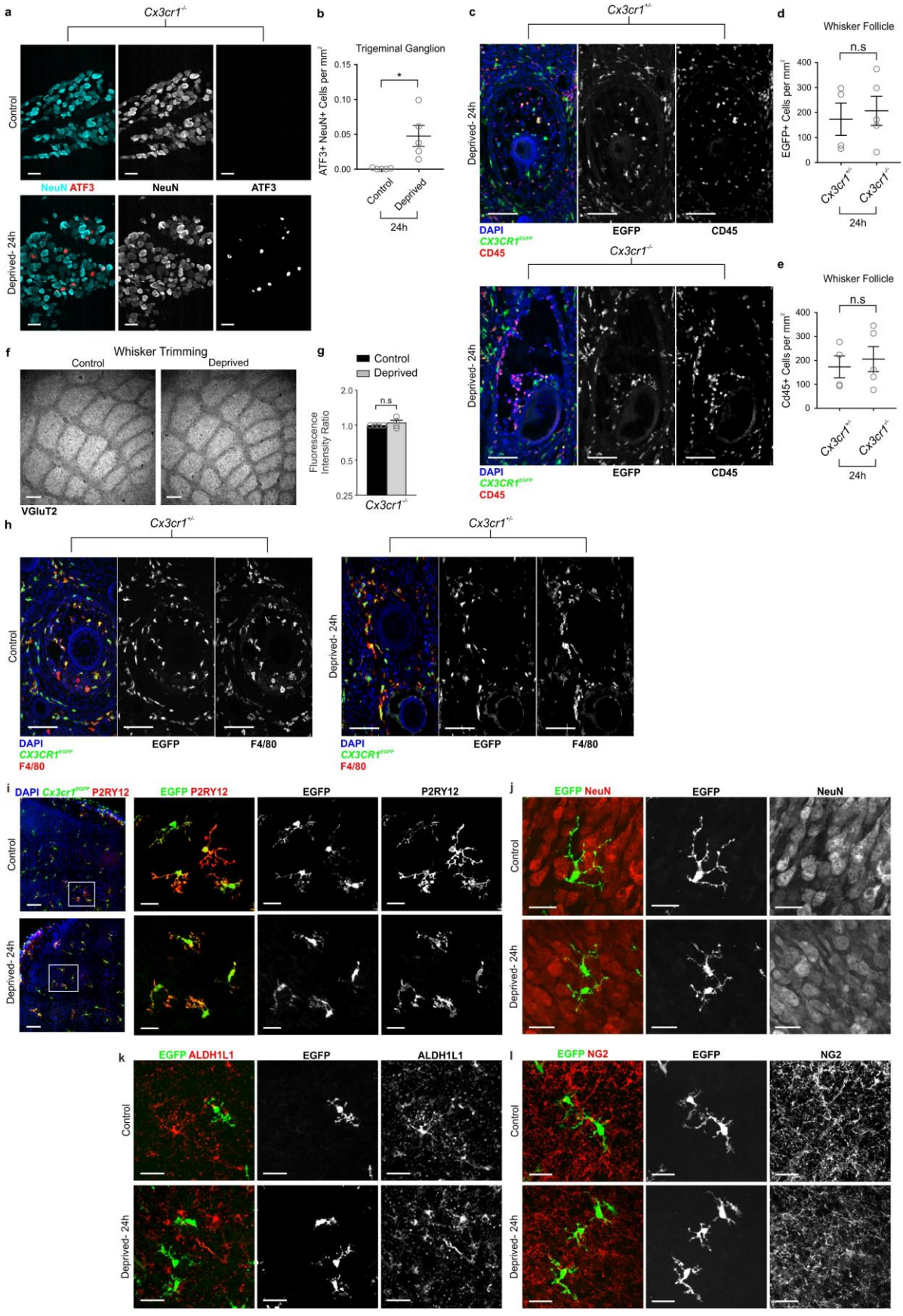
a
Cx3cr1+/-
Control
Deprived- 24h
NeuN ATF3
NeuN
ATF3
b
Trigeminal Ganglion
ATF3+ NeuN+ Cells per mm2
0.15
0.10
0.05
0.00
*
Control
Deprived
24h
c
Cx3cr1+/-
Deprived- 24h
DAPI
CX3CR1EGFP
CD45
EGFP
CD45
Cx3cr1-/-
d
Whisker Follicle
n.s
EGFP+ Cells per mm2
400
300
200
100
0
Cx3cr1+/-
Cx3cr1-/-
24h
e
Whisker Follicle
n.s
Cd45+ Cells per mm2
400
300
200
100
0
Cx3cr1+/-
Cx3cr1-/-
24h
f
Whisker Trimming
Control
Deprived
VGluT2
g
Control
Deprived
Fluorescence Intensity Ratio
2.0
1.0
0.5
0.25
n.s
Cx3cr1-/-
h
Cx3cr1+/-
Control
Deprived- 24h
DAPI
CX3CR1EGFP
F4/80
EGFP
F4/80
i
DAPI Cx3cr1EGFP P2RY12
EGFP P2RY12
EGFP
P2RY12
Control
Deprived- 24h
j
EGFP NeuN
EGFP
NeuN
Control
Deprived- 24h
k
EGFP ALDH1L1
EGFP
ALDH1L1
Control
Deprived- 24h
l
EGFP NG2
EGFP
NG2
Control
Deprived- 24h

Supplementary Figure 5

Whisker lesioning in *Cx3cr1*$^{-/-}$ animals results in similar cell stress response and wound healing at the whisker follicles compared to *Cx3cr1*$^{+/+}$ animals.

a-b, Whisker lesioning increases ATF3 signal in the ipsilateral trigeminal nerve ganglion of *Cx3cr1*$^{-/-}$ animals (deprived, bottom panels, compare to Supplementary Figure 2a). Nuclei positive for ATF3 (red) are co-localized to NeuN signal (cyan). Scale bar, 50 µm. (Two-tailed Student's t-Test, $P = 0.0152$, $t = 3.362$, $df = 6$; n = 5 animals). **c-e,** Whisker lesioning in *Cx3cr1*$^{-/-}$ mice (bottom panels) results in similar wound healing response as measured by recruitment of CX3CR1-EGFP-positive (d; Two-tailed Student's t-Test, $P = 0.7115$, $t = 0.3852$, $df = 7$; n = 4 *Cx3cr1*$^{+/-}$, 5 *Cx3cr1*$^{-/-}$ animals) and CD45 macrophages/monocytes (e; Two-tailed Student's t-Test, $P = 0.6656$, $t = 0.4511$, $df = 7$; n = 4 *Cx3cr1*$^{+/-}$, 5 *Cx3cr1*$^{-/-}$ animals) compared to *Cx3cr1*$^{+/+}$ animals (top panels) 24 hours after injury. Scale bars, 100 µm. Data presented as mean ± SEM. **f-g,** Whisker trimming in *Cx3cr1*$^{-/-}$ animals from P4 to P20 (16 days deprivation) does not result in a decrease in barrel fluorescence intensity (compare to Supplementary Figure 1a-b). Top panel, control barrel field fluorescence; bottom panel, deprived barrel field fluorescence at P20. Representative images taken from 4 animals. Quantification for fluorescence intensity (g) does not show a significant decrease in fluorescence (Two-tailed Student's t-test, n = 4 animals, $P = 0.3455$, $t = 1.024$, $df = 6$). Data presented as mean ± SEM. **h**, *Cx3cr1* expression is specific to peripheral macrophages and monocytes in the whisker follicles and surrounding tissue before (left panels) and after (right panels) whisker lesioning in a *Cx3cr1*$^{+/-}$ animal. *Cx3cr1EGFP* expression (EGFP, green) is co-localized with macrophage marker F4/80 (red) in both control and cauterized follicles. Scale bars, 100 µm. Representative images taken from 9 animals (n = 4 *Cx3cr1*$^{+/-}$, 5 *Cx3cr1*$^{-/-}$ animals). **i-l**, *Cx3cr1* expression is specific to microglia both before (control, top panels) and 24 hours after (deprived, bottom panels) whisker lesioning in the primary somatosensory cortex. *Cx3cr1EGFP* expression is specific to microglia (**i,** P2RY12, low magnification scale bars 80 µm, high magnification scale bars 25 µm) but not neuronal (**j**, NeuN, scale bars 25 µm), astrocyte (**k**, ALDH1L1, scale bars 25 µm), or oligodendrocyte precursor (**l**, NG2, scale bars 25 µm) specific markers. Representative images taken from 3 *Cx3cr1*$^{+/-}$ animals.

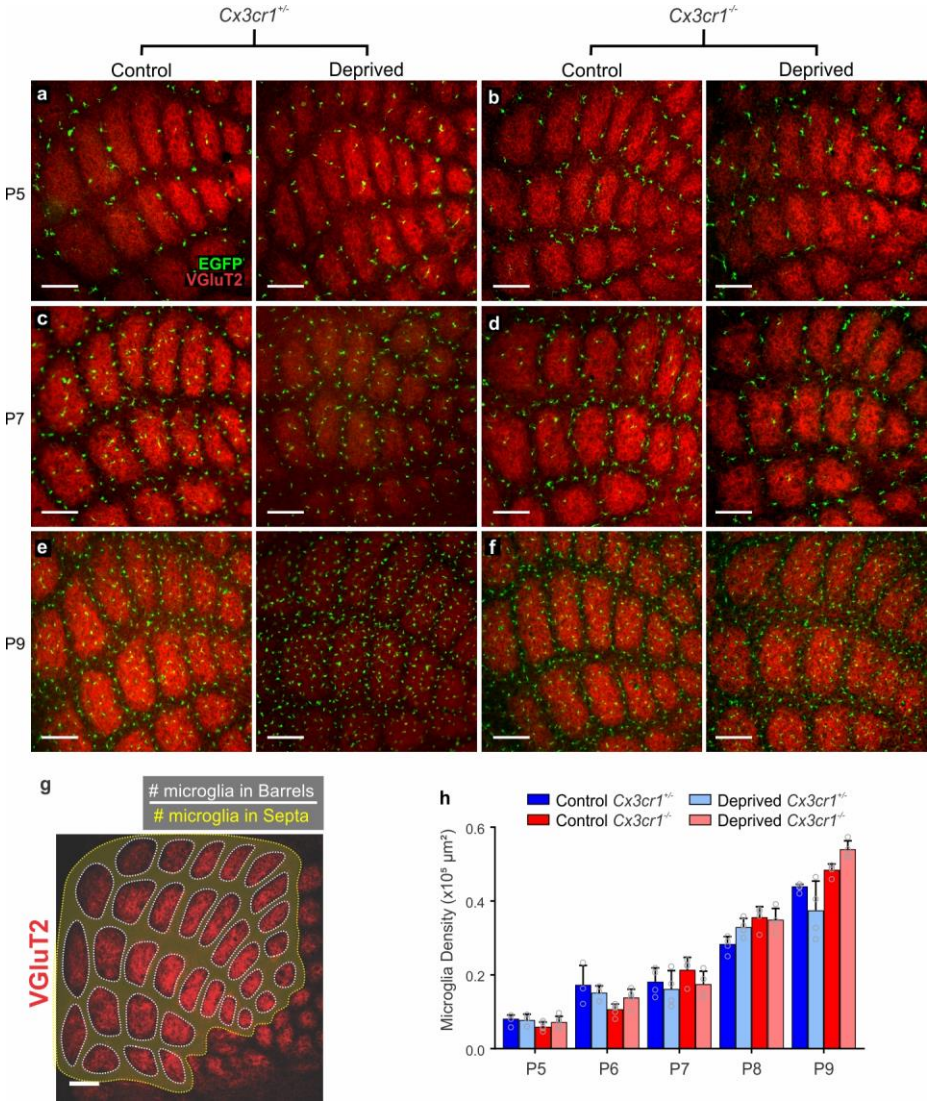

Supplementary Figure 6

Total number of microglia across the barrel field increases with postnatal age and is similar in *Cx3cr1*$^{+/-}$ and *Cx3cr1*$^{-/-}$ mice.

a-f, Uncropped images of microglia recruitment to barrel centers from Figure 5. Scale bar, 150 µm. Representative images taken from 11 animals. **g,** For each genotype, the number of microglia within the septa (yellow highlighted area) and barrels (outlined by white dotted lines) were quantified in deprived and control, non-deprived layer IV barrel cortices. A ratio was then calculated: # of microglia within the barrel divided by the # of microglia within the septa. Scale bar, 150 µm. **h**, For each postnatal age analyzed, the total microglial cell density over the entire layer IV primary somatosensory cortex is not significantly changed between *Cx3cr1*$^{+/-}$ and *Cx3cr1*$^{-/-}$ mice. (Two-Way ANOVA with Dunnett's post hoc test, n=4 animals per genotype; for P5: control +/- vs deprived +/-, $P = 0.9997$, $q = 0.06821$, $df = 60$, control +/- vs control -/-, $P = 0.9371$, $q = 0.4673$, $df = 60$, control +/- vs deprived -/-, $P = 0.9949$, $q = 0.1929$, $df = 60$; for P6: control +/- vs deprived +/-, $P = 0.9549$, $q = 0.4136$, $df = 60$, control +/- vs control -/-, $P = 0.3484$, $q = 1.436$, $df = 60$, control +/- vs deprived -/-, $P = 0.7974$, $q = 0.7459$, $df = 60$; for P7: control +/- vs deprived +/-, $P = 0.9468$, $q = 0.4392$, $df = 60$, control +/- vs control -/-, $P = 0.8091$, $q = 0.7266$, $df = 60$, control +/- vs deprived -/-, $P = 0.9979$, $q = 0.1442$, $df = 60$; for P8: control +/- vs deprived +/-, $P = 0.5973$, $q = 1.043$, $df = 60$, control +/- vs control -/-, $P = 0.2481$, $q = 1.639$, $df = 60$, control +/- vs deprived -/-, $P = 3.194$, $q = 1.490$, $df = 60$; for P9: control +/- vs deprived +/-, $P = 0.3258$, $q = 1.479$, $df = 60$, control +/- vs control -/-, $P = 0.6219$, $q = 1.008$, $df = 60$, control +/- vs deprived -/-, $P = 0.0694$, $q = 2.269$, $df = 60$). All data presented as mean ± SEM.

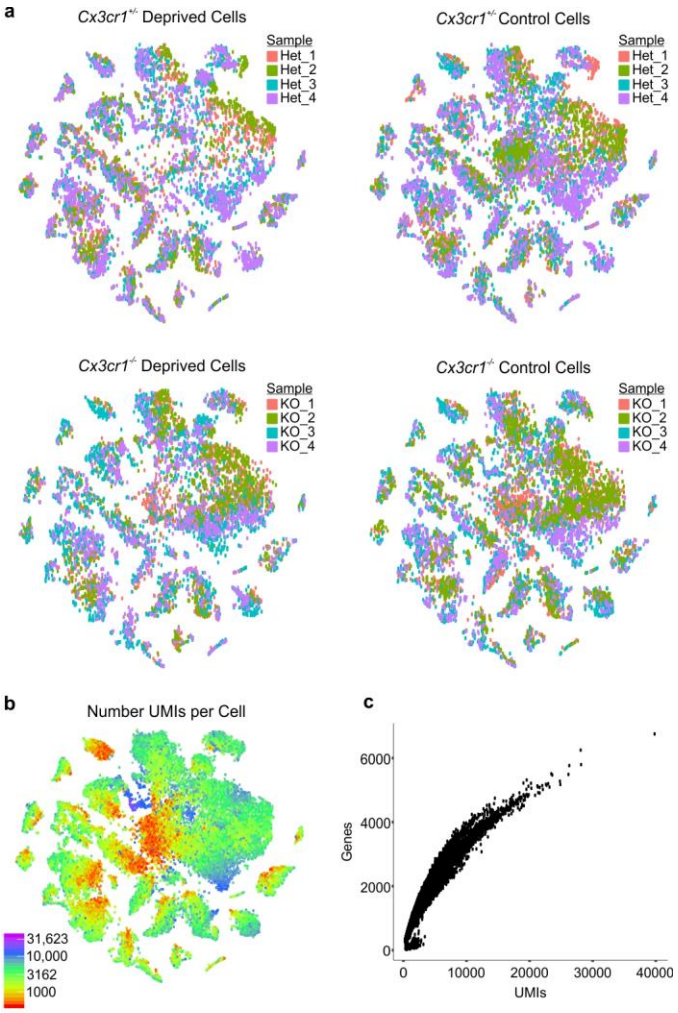

d	Reads	Reads with unique alignment	Reads with no alignments	UMIFM
Mouse01	5131.28	2952.705359	1962.24287	1642.79
Mouse02	7192.32	3777.569744	3162.182974	1893.78
Mouse03	7324.4	4413.287984	2663.654332	1881.9
Mouse04	7508.27	4705.885216	2555.412059	1605.41
Mouse05	8392.64	4515.337675	3557.100172	2192.74
Mouse06	3701.45	2298.715843	1261.619289	1526.6
Mouse07	9334.52	5821.114634	3206.723902	2346.93
Mouse08	5222.92	3202.010429	1843.785889	1687.41
Mouse09	12628.7	8791.609852	3401.364916	3276.6
Mouse10	11396.9	7830.870018	3153.854077	3031.85
Mouse11	8884.22	6360.826473	2210.066183	2783.4
Mouse12	14058	9797.345388	3786.499526	3215.88
Mouse13	13746.8	9685.512426	3605.394877	3499.86
Mouse14	11478.6	8073.456325	3011.768951	3179.17
Mouse15	4042.12	2758.699306	1134.021612	1960.2
Mouse16	11004.2	7639.631287	3006.15713	3021.2

Supplementary Figure 7

Biological replicate contribution and sequencing depth of cells captured by inDrops.

a, Clustering cells from each animal condition across n = 4 *Cx3cr1*$^{+/-}$ and n = 4 *Cx3cr1*$^{-/-}$ animals reveals even distribution of cells from each animal across all identified cell populations. Each tSNE plot represents cells from each animal genotype and condition (*Cx3cr1*$^{+/-}$ control, *Cx3cr1*$^{+/-}$ deprived, *Cx3cr1*$^{-/-}$ control, *Cx3cr1*$^{-/-}$ deprived). **b**, The number of unique molecular identifiers (UMIs) per cell processed by inDrops single-cell RNAseq (logarithmic scale) across n = 4 *Cx3cr1*$^{+/-}$ and n = 4 *Cx3cr1*$^{-/-}$ animals. **c**, The number of genes positively identified increases with increasing UMIs. **d**, Table containing average number of reads per cell across individual animals.

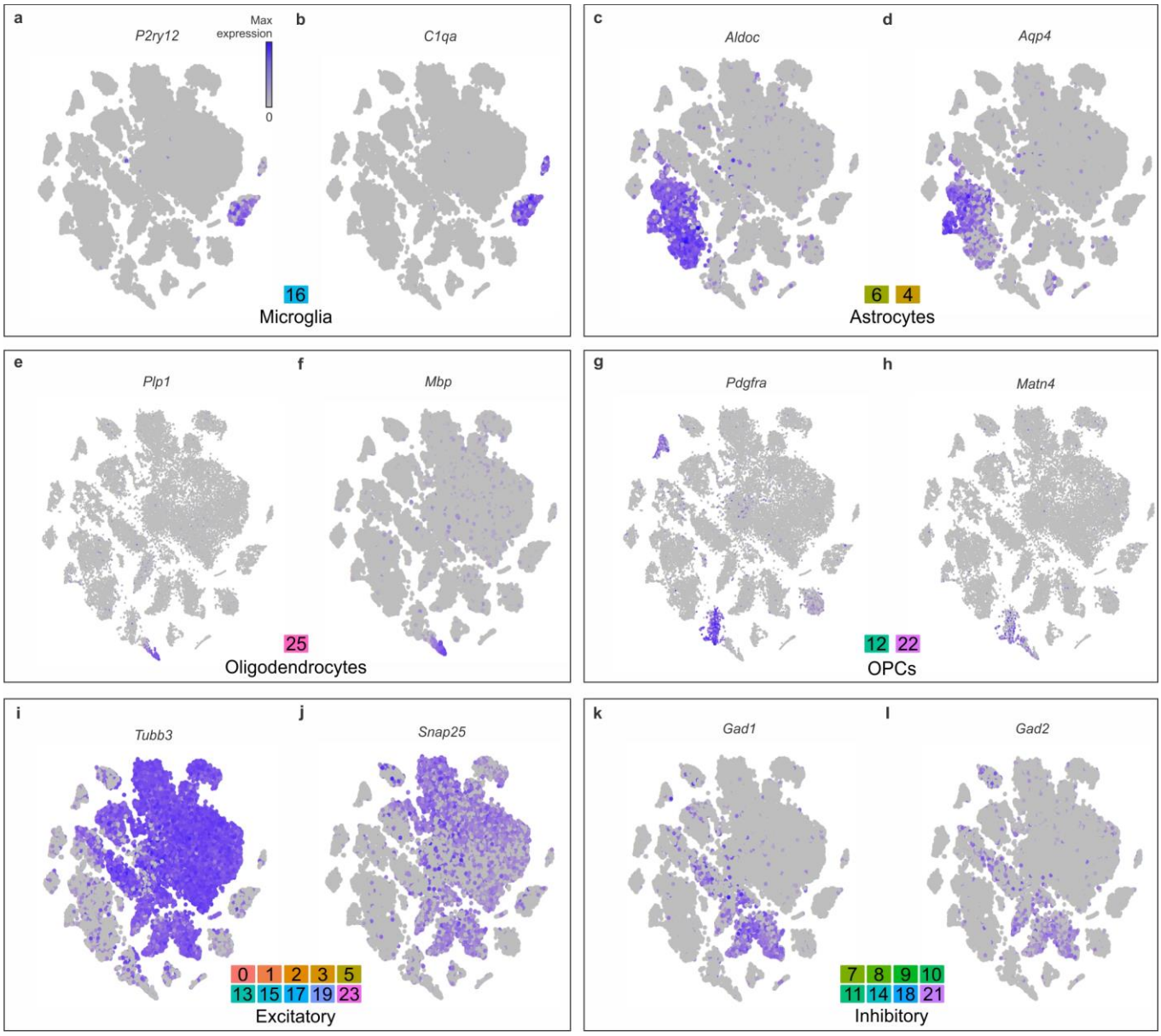

Supplementary Figure 8

Cell populations clustered through principal component analysis were identified according to specific cell-type markers.

a-b, Microglia cluster identified by *P2ry12* and *C1qa*. **c-d**, Astrocyte clusters identified by *Aldoc* and *Aqp4* expression. **e,f**, Oligodendrocyte cluster identified by *Plp1* and *Mpb* expression. **e-f**, Oligodendrocyte precursor cell clusters identified by *Pdgfra* and *Matn4* expression. **i-j**, Neuron clusters identified by *Tubb3* and *Snap25* expression. **k-l**, Inhibitory neurons identified by *Gad1* and *Gad2* expression. All cells represented across n = 4 *Cx3cr1*$^{+/-}$ and n = 4 *Cx3cr1*$^{-/-}$ animals.

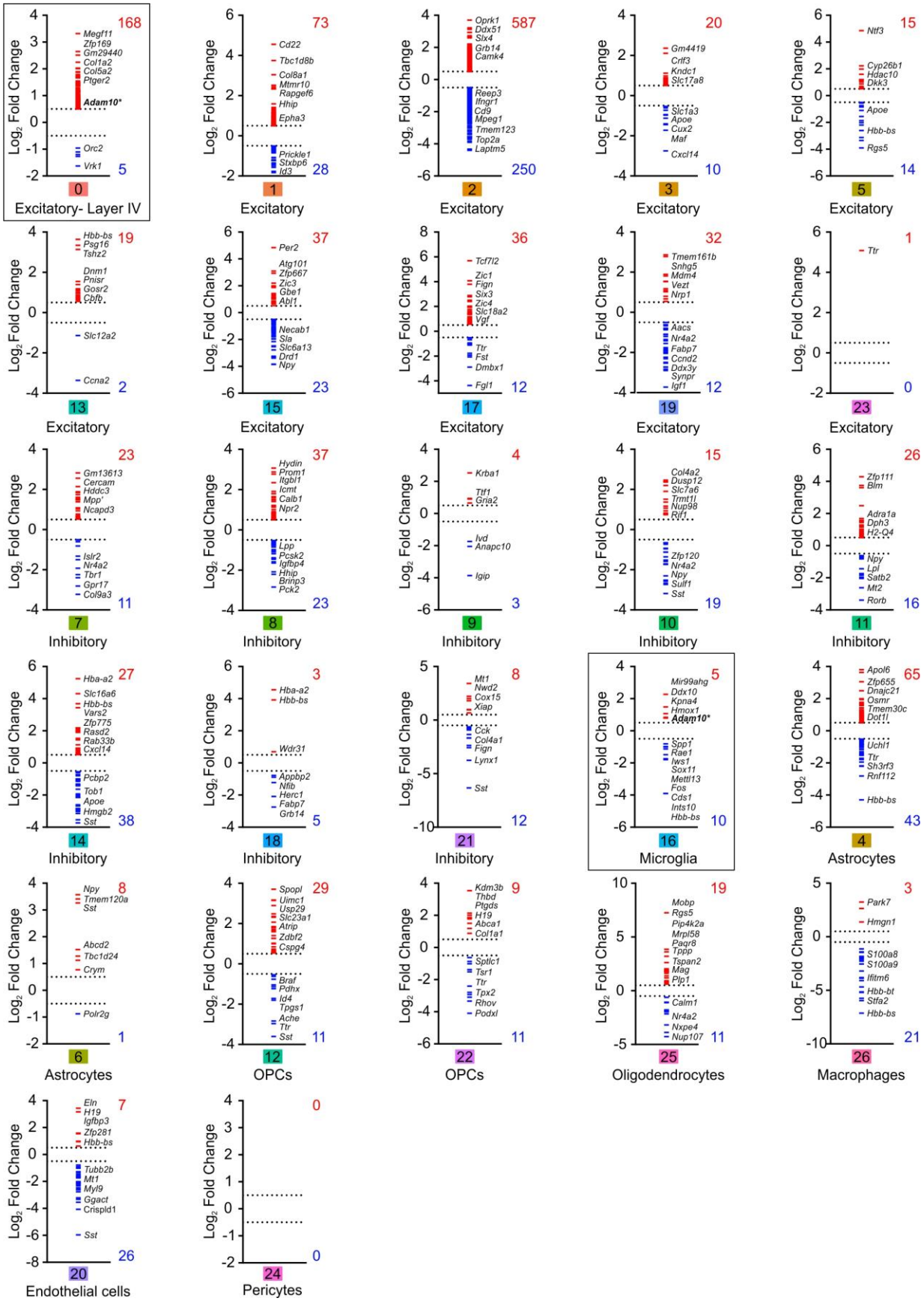
Log2 Fold Change
168
Megf11
Zfp169
Gm29440
Col1a2
Col5a2
Ptger2
Adam10*
Orc2
Vrk1
5
0
Excitatory- Layer IV
73
Cd22
Tbc1d8b
Col8a1
Mtmr10
Rapgef6
Hhip
Epha3
Prickle1
Stxbp6
Id3
28
1
Excitatory
587
Oprk1
Ddx51
Stx4
Grb14
Camk4
Reep3
Ifngr1
Cd9
Mpeg1
Tmem123
Top2a
Laptm5
250
2
Excitatory
20
Gm4419
Crlf3
Kndc1
Slc17a8
Slc1a3
Apoe
Cux2
Maf
Cxcl14
10
3
Excitatory
15
Ntf3
Cyp26b1
Hdac10
Dkk3
Apoe
Hbb-bs
Rgs5
14
5
Excitatory
19
Hbb-bs
Psg16
Tshz2
Dnm1
Pnisr
Gosr2
Cbfb
Slc12a2
Ccna2
2
13
Excitatory
37
Per2
Atg101
Zfp667
Zic3
Gbe1
Abl1
Necab1
Sla
Slc6a13
Drd1
Npy
23
15
Excitatory
36
Tcf7l2
Zic1
Fign
Six3
Zic4
Slc18a2
Vgf
Ttr
Fst
Dmbx1
Fgl1
12
17
Excitatory
32
Tmem161b
Snhg5
Mdm4
Vezt
Nrp1
Aacs
Nr4a2
Fabp7
Ccnd2
Ddx3y
Synpr
Igf1
12
19
Excitatory
1
Ttr
0
23
Excitatory
23
Gm13613
Cercam
Hddc3
Mpp'
Ncapd3
Islr2
Nr4a2
Tbr1
Gpr17
Col9a3
11
7
Inhibitory
37
Hydin
Prom1
Itgbl1
Icmt
Calb1
Npr2
Lpp
Pcsk2
Igfbp4
Hhip
Bnip3
Pck2
23
8
Inhibitory
4
Krba1
Ttf1
Gria2
Ivd
Anapc10
Igip
3
9
Inhibitory
15
Col4a2
Dusp12
Slc7a6
Trmt1l
Nup98
Rif1
Zfp120
Nr4a2
Npy
Sulf1
Sst
19
10
Inhibitory
26
Zfp111
Blm
Adra1a
Dph3
H2-Q4
Npy
Lpl
Satb2
Mt2
Rorb
16
11
Inhibitory
27
Hba-a2
Slc16a6
Hbb-bs
Vars2
Zfp775
Rasd2
Rab33b
Cxcl14
Pcbp2
Tob1
Apoe
Hmgb2
Sst
38
14
Inhibitory
3
Hba-a2
Hbb-bs
Wdr31
Appbp2
Nfib
Herc1
Fabp7
Grb14
5
18
Inhibitory
8
Mt1
Nwd2
Cox15
Xiap
Cck
Col4a1
Fign
Lynx1
Sst
12
21
Inhibitory
5
Mir99ahg
Ddx10
Kpna4
Hmox1
Adam10*
Spp1
Rae1
Iws1
Sox11
Mettl13
Fos
Cds1
Ints10
Hbb-bs
10
16
Microglia
65
Apol6
Zfp655
Dnajc21
Osmr
Tmem30c
Dot1l
Uchl1
Ttr
Sh3rf3
Rnf112
Hbb-bs
43
4
Astrocytes
8
Npy
Tmem120a
Sst
Abcd2
Tbc1d24
Crym
Polr2g
1
6
Astrocytes
29
Spopl
Uimc1
Usp29
Slc23a1
Atrip
Zdbf2
Cspg4
Braf
Pdhx
Id4
Tpgs1
Ache
Ttr
Sst
11
12
OPCs
9
Kdm3b
Thbd
Ptgds
H19
Abca1
Col1a1
Sptlc1
Tsr1
Ttr
Tpx2
Rhov
Podxl
11
22
OPCs
19
Mobp
Rgs5
Pip4k2a
Mrpl58
Paqr8
Tppp
Tspan2
Mag
Plp1
Calm1
Nr4a2
Nxpe4
Nup107
11
25
Oligodendrocytes
3
Park7
Hmgn1
S100a8
S100a9
Ifitm6
Hbb-bt
Stfa2
Hbb-bs
21
26
Macrophages
7
Eln
H19
Igfbp3
Zfp281
Hbb-bs
Tubb2b
Mt1
Myl9
Ggact
Crispld1
Sst
26
20
Endothelial cells
0
0
24
Pericytes

Supplementary Figure 9

Genes significantly changed for each cell population in the deprived cortex of *Cx3cr1*$^{+/-}$ animals.

Genes with significant changes in expression (FDR <0.10) and Log_2 Fold Change greater than 0.5 or less than -0.5 in the deprived cortex for n = 4 *Cx3cr1*$^{+/-}$ are plotted for every identified cell population (Monocle2). Note ADAM10 (bold text and asterisks) is only significantly increased in layer IV excitatory neurons and microglia (outlined graphs).

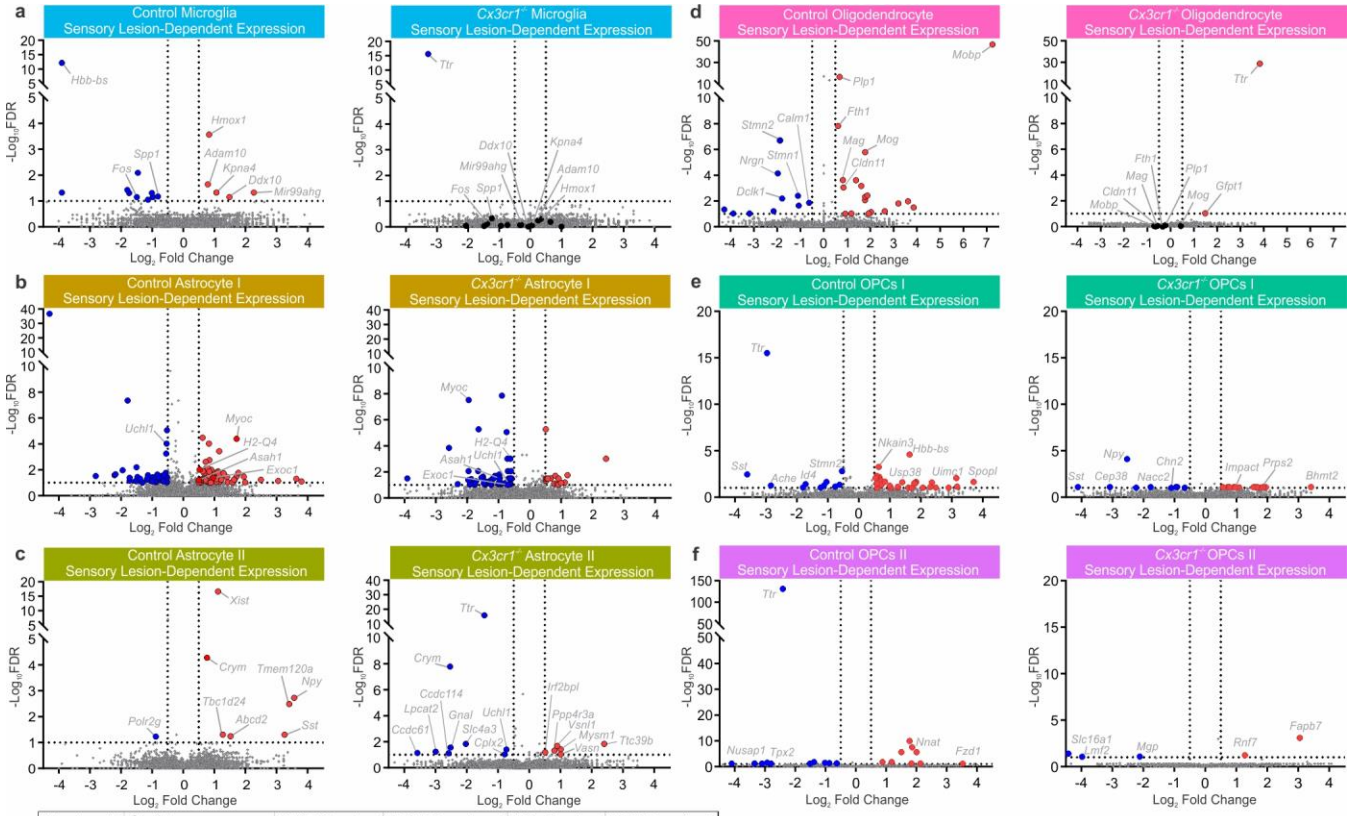

g

Cluster #	Cell type	HET Control	HET Deprived	KO Control	KO Deprived
0	Excitatory	783	549	847	803
1	Excitatory	773	459	946	804
2	Excitatory	1135	415	873	438
3	Excitatory	697	562	781	724
4	Astrocytes	668	671	554	519
5	Excitatory	393	245	563	448
6	Astrocytes	445	474	348	346
7	Inhibitory	382	324	465	343
8	Inhibitory	411	392	329	362
9	Inhibitory	490	476	269	242
10	Inhibitory	422	368	309	275
11	Inhibitory	343	281	313	232
12	OPCs	290	311	209	197
13	Excitatory	258	241	209	230
14	Inhibitory	235	260	270	123
15	Excitatory	165	184	292	234
16	Microglia	264	282	166	116
17	Excitatory	180	287	195	37
18	Inhibitory	188	180	188	99
19	Excitatory	109	180	161	203
20	Endothelial Cells	109	182	145	117
21	Inhibitory	87	112	211	84
22	OPCs	89	169	65	73
23	Excitatory	80	83	134	99
24	Pericytes	116	153	55	55
25	Oligodendrocytes	96	109	58	47
26	Macrophages	64	78	53	33
27	Unknown	62	60	23	59
	SUM	9334	8087	9031	7342

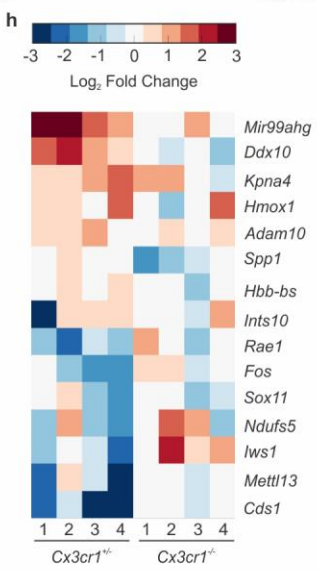

Supplementary Figure 10

Sensory-lesion dependent gene expression changes in all major glial cell populations in the deprived cortices of *Cx3cr1*$^{+/-}$ and *Cx3cr1*$^{-/-}$ animals.

a, Gene expression changes for *Cx3cr1*$^{+/-}$ microglia (left panel, from n = 4 *Cx3cr1*$^{+/-}$ animals) and *Cx3cr1*$^{-/-}$ microglia (right panel, from n = 4 *Cx3cr1*$^{-/-}$ animals). Dotted lines indicates –log$_{10}$FDR <0.10 and Log$_2$ Fold Change > 0.5 and < -0.5 (Monocle2). **b-f,** Gene

expression changes for all other identified glial cell types (Monocle2). **g,** Table containing the number of cells sequenced for each cell type for each animal genotype and condition. **h**, Heatmap for the Log_2Fold Change for microglial genes changed across n = 4 *Cx3cr1*$^{+/-}$ and n = 4 *Cx3cr1*$^{-/-}$ animals hierarchically clustered by variable gene expression for *Cx3cr1*$^{+/-}$ samples (Monocle2).

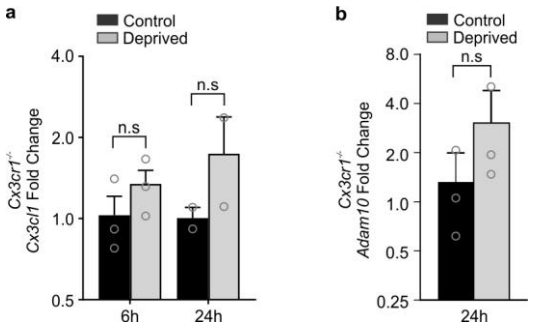

Supplementary Figure 11

qPCR in *Cx3cr1*$^{-/-}$ primary somatosensory cortex reveals no significant increase in *Cx3cl1* nor *Adam10* expression after whisker lesioning.

a, Quantification for *Cx3cl1* expression 6h and 24h post lesioning. (Two-way ANOVA with Sidak's post hoc, 6h control vs deprived P = 0.6640, t = 0.8648, df = 6; 24h control vs deprived P = 0.2808, t = 1.641, df = 6; n = 3 animals per timepoint). **b**, Quantification for *Adam10* expression 24h post lesioning. (Two-tailed Student's t-Test, P = 0.4414, t = 0.9099, df = 4; n = 3 animals). Data presented as mean ± SEM.

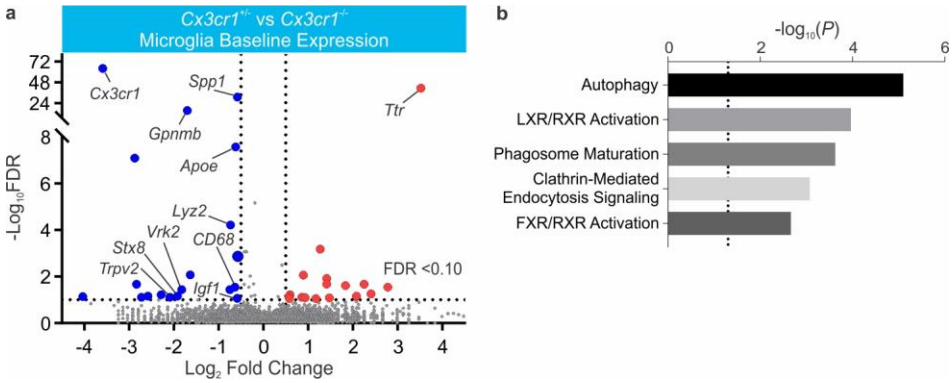

Supplementary Figure 12

Baseline expression in *Cx3cr1*$^{-/-}$ microglia reveals significant changes in genes related to phagocytic signaling.

a, Volcano plot of genes significantly downregulated (fold change < -0.5, FDR <0.10, p<0.0005, Monocle2) in *Cx3cr1*$^{-/-}$ microglia within the non-deprived, control barrel cortex compared to *Cx3cr1*$^{+/-}$ littermates reveals several genes are dysregulated basally in *Cx3cr1*$^{-/-}$ microglia. (Microglia from n = 4 *Cx3cr1*$^{+/-}$ and n = 4 *Cx3cr1*$^{-/-}$ animals). **b**, Gene ontology clustering of genes in *Cx3cr1*$^{-/-}$ microglia (Dotted line, p<0.05) reveals several genes related to phagocytic signaling are significantly changed (single cell performed on n = 4 *Cx3cr1*$^{+/-}$ and n = 4 *Cx3cr1*$^{-/-}$ animals yielding 828 microglia, see also Supplementary Figure 9g). Data analyzed through the use of IPA (QIAGEN Inc., https://www.qiagenbioinformatics.com/products/ingenuitypathway-analysis).